Available online at www.sciencedirect.com
SCIENCE DIRECT®
Journal of Power Sources 125 (2004) 77–84
JOURNAL OF POWER SOURCES
www.elsevier.com/locate/jpowsour

Microwave synthesis and electrochemical properties of $LiCo_{1-x}M_xO_2$ (M = Al and Mg) cathodes for Li-ion rechargeable batteries

P. Elumalai [a], H.N. Vasan [a,*], N. Munichandraiah [b]

[a] *Solid State and Structural Chemistry Unit, Indian Institute of Science, Bangalore 560012, India*
[b] *Department of Inorganic and Physical Chemistry, Indian Institute of Science, Bangalore 560012, India*

Received 5 May 2003; accepted 8 July 2003

Abstract

Single phase $LiCo_{1-x}M_xO_2$ (M = Al and Mg) cathode materials for Li-ion batteries are synthesized by microwave dielectric heating with a reaction time less than 20 min. Aluminium forms solid solutions up to a composition of $x = 0.5$ and magnesium up to $x = 0.2$. Lattice constants are found to vary with the composition. The compounds are electrochemically active with good discharge capacity.

Keywords: Li-ion battery; Cathodes; Aluminum and magnesium substitution; Microwave synthesis; Discharge capacity

1. Introduction

Lithium-ion rechargeable batteries that have high specific energy and long cycle-life are useful for a variety of application [1]. The Li-ion battery consists of lithiated carbon as the anode, lithium transition metal oxide of formula $LiMO_2$ (M = Co, Ni) or $LiMn_2O_4$ as the cathode, and a Li-salt dissolved in a non-aqueous medium as the electrolyte. Among the lithium transition metal oxides that have a α-$NaFeO_2$ structure, $LiCoO_2$ has been widely used as a cathode material [2]. The high cost and toxicity of Co, however, makes the use of $LiCoO_2$ undesirable. In order to reduce the cost and to improve the cell voltage and specific energy, other transition metals such as Cr [3], Mn [4], Fe [5–7], Ni [7–9] and Rh [10] are used to partially substitute Co in $LiCoO_2$. Non-transition metals such as Al and Mg, which have fixed oxidation states, may also be used to partially substitute Co. Ceder et al. [11] have predicted, from first principles and also shown by experiment, that substitution of Al increases the potential as well as the performance of $LiCoO_2$. Consequent to this theoretical prediction, several studies of the substitution of Co by Al have been reported [11–19]. As Mg is lightweight and cheap, it has also been considered as a substituent for Co. By contrast, there have been very few investigations of Mg substitution [20]. In all these studies, the $LiCo_{1-x}M_xO_2$ (M = Al and Mg) compounds have been synthesized by conventional ceramic methods [12,14–20] and thin films by pulsed laser ablation technique [13,21].

Conventional methods for the synthesis of $LiCoO_2$ and doped compounds are tedious and time-consuming, often extending to several days [22,23]. A few fast and easy methods of synthesis have been briefly reviewed, and a low-temperature solution combustion method has been reported recently by Rodrigues et al. [24]. There has been a growing interest in using microwave heating for sintering ceramics following disclosure of this technique by Berteaud and Badot [25], for the sintering of alumina and silica. Microwave dielectric heating has also been used to prepare superconductors, carbides and borides [26–28]. This procedure involves the absorption of microwave radiation directly or indirectly by the reactants, which results in rapid heating, forming the desired products in a very short time. Thus synthesis becomes very economical and clean [29,30].

Recently, microwave heating has been employed for the preparation of cathode materials for Li-ion batteries [31–34]. For example, Whitfield and Davidson [33] have synthesized $LiMn_2O_4$ starting from various manganese oxides and LiOH. From Li_2CO_3 and Co_3O_4, Subramanian et al. [34] prepared $LiCoO_2$. To the authors knowledge, however, microwave synthesis of $LiCo_{(1-x)}M_xO_2$ (M = Al and Mg) compounds and their electrochemical properties have not been reported. We have been involved in the preparation

* Corresponding author. Tel.: +91-80-2932951/2932295; fax: +91-80-3601310.
E-mail address: vasan@sscu.iisc.ernet.in (H.N. Vasan).

0378-7753/$ – see front matter © 2003 Elsevier B.V. All rights reserved.
doi:10.1016/S0378-7753(03)00815-2

of several cathode materials using microwave synthesis and the preliminary studies based on $LiCo_{1-x}Ni_xO_2$ have been reported recently [35]. This study examines the microwave synthesis of Al and Mg substituted $LiCoO_2$ compounds and their electrochemical performance for Li-ion batteries.

2. Experimental

For synthesis of $LiCo_{1-x}M_xO_2$ (M = Al and Mg), the required mole concentration of cobalt, magnesium and aluminium nitrates (all AR grade S.D. Fine Chemicals, India) were taken to obtain a final product of about 3.0 g. The components were mixed and dissolved in a minimum amount of distilled water. To this, twice the mole concentration of $LiOH{\cdot}2H_2O$ (AR grade S.D. Fine Chemicals, India) was added and mixed in a 50 ml porcelain crucible. Excess of LiOH was used to compensate for the Li as Li_2O during the reaction. The crucible was covered with a lid and kept in a beaker placed at the centre of a rotating plate of an unmodified kitchen microwave oven (BPL-Sanyo, India, 2.5 GHz 850 W). The crucible was irradiated for 15 min at 50% power, and then for 5 min at 100% power. During this period, it was observed that the chemical constituents were rapidly heated and a red glow was seen inside the crucible throughout the reaction. After reaction, the product was allowed to cool to room temperature. At this stage, X-ray diffraction (XRD) analysis was undertaken and showed the presence of a small amount of Li_2CO_3, which was removed by thorough washing with methanol. The final product was characterized by means of power XRD using a Co source ($\lambda = 1.7902$ Å) in a JEOL JDX-8P X-ray diffractometer, and by scanning electron microscopy using a JEOL JSM/840A microscope. Several samples of $LiCo_{1-x}Al_xO_2$ ($0 \le x \le 0.6$) and $LiCo_{1-x}Mg_xO_2$ ($0 \le x \le 0.2$) were prepared. For electrochemical characterization, oxide electrodes were prepared on an aluminium foil as the substrate. The foil had a rectangular shape (2.5 cm × 0.5 cm) and a tag for electrical connections. The foil was polished with successive grades of emery paper to a uniform and smooth finish, cleaned with detergent, washed copiously with double-distilled water, rinsed with acetone, and finally dried in air.

$LiCo_{1-x}M_xO_2$ (65 wt.%), acetylene black (25 wt.%) and PVDF (10 wt.%) with a total weight of about 0.1 g were mixed with a minimum volume of *n*-methylpyrolidinone (NMP) to form a syrupy mixture. The mixture was repeatedly spread on to the aluminium foil so as to obtain a uniform coating, and finally dried at 393 K for about 12 h under vacuum. The electrodes thus prepared were compacted at 25 kN cm^{-2} pressure and heated again for 6 h at 393 K prior to transferring into an argon-filled dry box. Cells were assemble in polypropylene containers in a two-electrode configuration with lithium metal as the counter electrode. A polypropylene microporous film (Celgard) was used as the inter-electrode separator. The electrolyte consisted of 1 M $LiBF_4$ in an ethylene carbonate (EC) and dimethyl carbonate (DMC) mixture (1:1). The two solvents were earlier distilled three times in an argon atmosphere and repeatedly treated with 4 Å molecular sieves. Cyclic voltammetric experiments were performed by means of a EG&G PARC potentiostat/galvanostat (model Versastat). Electrochemical impedance spectra were measured in the frequency range 100 kHz to 10 mHz with an excitation signal of 5 mV by means of an EG&G PARC electrochemical impedance analyzer model 6390. Galvanostatic charge–discharge cycling data were obtained with a galvanostatic circuit that consisted of a regulated dc power source, a high resistance, and an ammeter in series with the cell. A digital multimeter of high input-impedance was used to measure the electrode potentials.

3. Results and discussions

3.1. Powder XRD and SEM

The powder XRD patterns of $LiCo_{1-x}Al_xO_2$ ($0 \le x \le 0.6$) and $LiCo_{1-x}Mg_xO_2$ ($0 \le x \le 0.3$) are shown in Figs. 1 and 2, respectively. It is seen that a single phase is formed for compositions up to $x = 0.5$ for Al substitution, and up to $x = 0.2$ for Mg substitution. The XRD patterns are indexed to a hexagonal unit cell with space group *R*3-*m* and an α-$NaFeO_2$ structure. It is interesting to note that as the Al content increases, the (0 0 6) and (1 0 8) peaks shift to higher '*d*' values, and the (1 1 0) peaks to lower '*d*' values, which leads to wider splitting of the (0 0 6)/(0 1 2) and (1 0 8)/(1 1 0) peaks compared with the parent compound $LiCoO_2$ and indicates a well-developed, layered, high-temperature (HT) phase. At compositions $x > 0.5$, γ-$LiAlO_2$ separates out as a phase, as seen in Fig. 1. Thus, the solubility of Al in $LiCoO_2$ is limited to $x = 0.5$. The formation of solid solutions is evidently reflected in the hexagonal lattice parameters. Lattice constants '*a*' and '*c*' were obtained by least-square refinements, and are shown in Fig. 3. It is seen distinctly that substitution of Al for Co in $LiCoO_2$ results in decrease in '*a*' and increase in '*c*' parameters. This phenomenon is due to shrinking of the inter-atomic distance within the CoO_2 layer, which results from the substitution of Co^{3+} by the smaller Al^{3+} ion. An interplanar expansion also exists due to an increase in columbic repulsion between CoO_2 layers. It is also clear that the *c*/*a* ratio increases as the Al content is increased (Fig. 3(c)), and the values are found to be >4.899. This suggests that Al-substituted samples are cationically well-ordered structures. These observations are in agreement with the literature [12,16].

Magnesium up to a composition of $x = 0.2$ forms a solid solution and the XRD patterns are also indexed to a hexagonal system with a *R*3-*m* space group, as seen in Fig. 2. For compositions beyond $x = 0.2$, it is a mixture of MgO and the layered compound. The formation of a solid solution is more pronounced with the hexagonal lattice parameters '*a*' and '*c*' (not shown) of the *R*3-*m* space group. It is observed

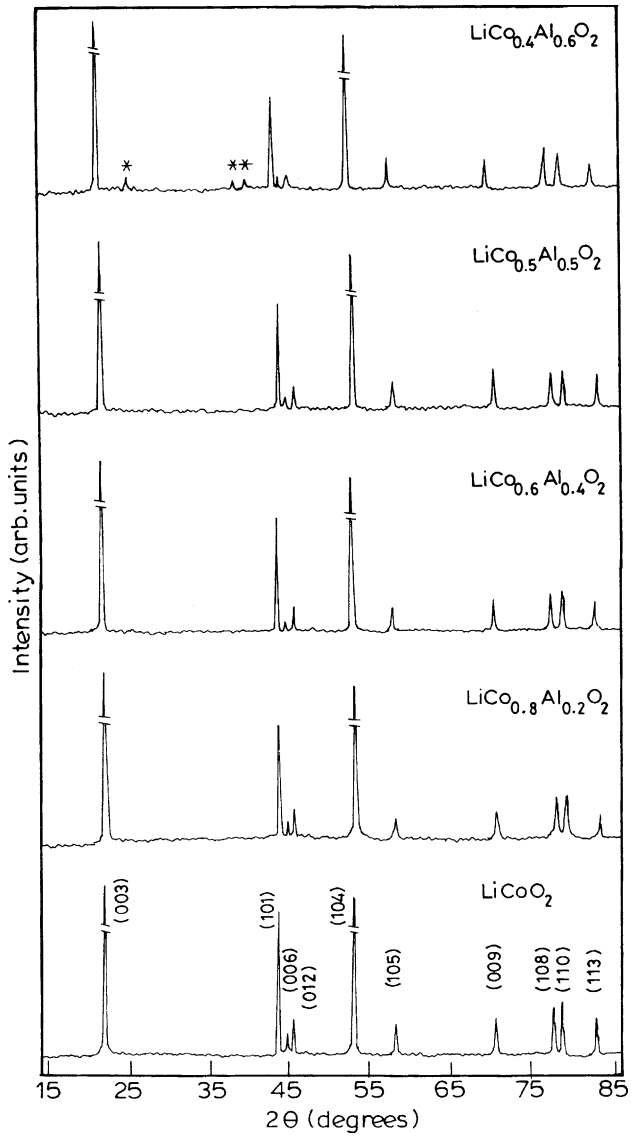

Fig. 1. Powder X-ray pattern for $LiCo_{1-x}Al_xO_2$ synthesized by microwave dielectric heating, indexed to hexagonal lattice: (*) denotes γ-$LiAlO_2$.

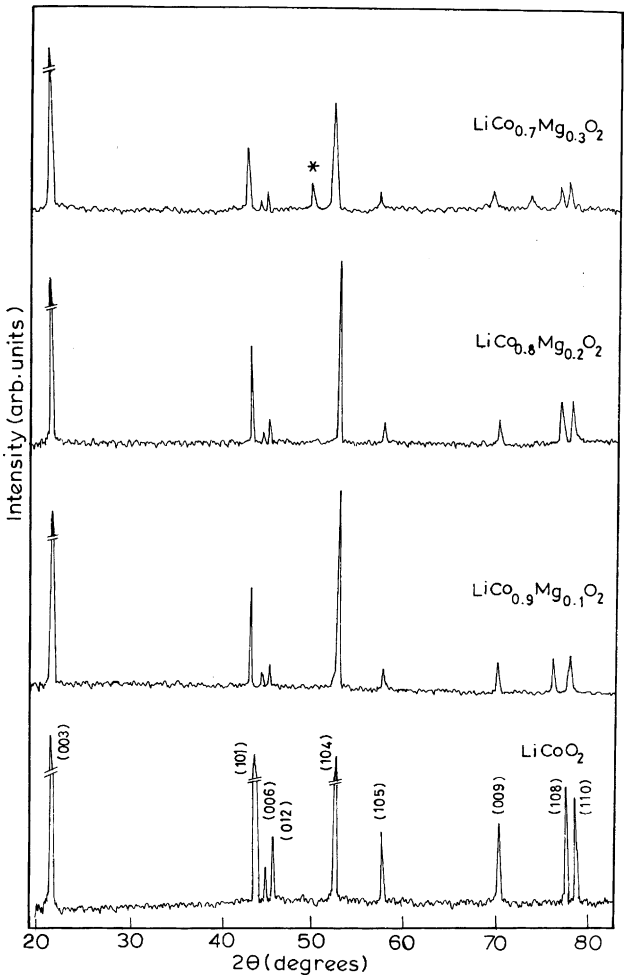

Fig. 2. Powder X-ray pattern for $LiCo_{1-x}Mg_xO_2$ synthesized by microwave dielectric heating, indexed to heaxagonal lattice: (*) denotes MgO.

that both the parameters increase with the substitution of Mg^{2+}, which is a significantly larger ion than Co^{3+}.

Representative scanning electron micrographs of $LiCoO_2$, $LiCo_{0.8}Al_{0.2}O_2$ and $LiCo_{0.9}Mg_{0.1}O_2$ samples are presented in Fig. 4. The particles are found to be crystalline with well-defined facets that have a wide range of distribution (1–10 μm). In the case $LiCo_{0.5}Al_{0.5}O_2$, however, the particles are smaller (<1 μm) and aggregated. Spot EDX taken on different crystallites reveals a uniform composition of Co, Al and Co, Mg, which confirms the global compositions.

3.2. Cyclic voltamograms and charge–discharge

In order to assess electrochemical activity, cyclic voltammograms of $LiCo_{1-x}Al_xO_2$ were recorded. The voltammogram of $LiCoO_2$ (Fig. 5(a)) shows an anodic current peak at 4.14 V and a cathodic peak at 3.72 V. There are also two weak cathodic peaks at 4.0 and 4.13 V, which may be due to an order–disorder transition of Li-ions in the CoO_2 framework, as reported by Dokko et al. [36]. The cyclic voltammograms of $LiCo_{1-x}Al_xO_2$ and $LiCo_{1-x}Mg_xO_2$ are similar to that of $LiCoO_2$ (Fig. 5). The weak cathodic peaks, however, are absent in the Al and Mg substituted $LiCoO_2$. These data qualitatively suggest that the compounds prepared by microwave assisted dielectric heating are electochemically active.

Further electrochemical characterization was carried out by galvanostatic charge–discharge studies between 3.0 and 4.2 V. Typical curves for $LiCoO_2$, $LiCo_{0.8}Al_{0.2}O_2$ and $LiCo_{0.9}Mg_{0.1}O_2$ are given in Fig. 6. On charging, the cell with $LiCoO_2$ (Fig. 6(a)) reaches a plateau at about 4.1 V. On discharging, a major part of the capacity is obtained at 3.9 V. In the case of $LiCoO_{1-x}Al_xO_2$, the discharge curves are steep, the steepness increases at higher values of x. It is seen that the efficiency of discharge–charge capacities is more than 80% in $LiCoO_2$, $LiCo_{0.8}Al_{0.2}O_2$ and $LiCo_{0.9}Mg_{0.1}O_2$, but is only about 50% in $LiCo_{0.5}Al_{0.5}O_2$.

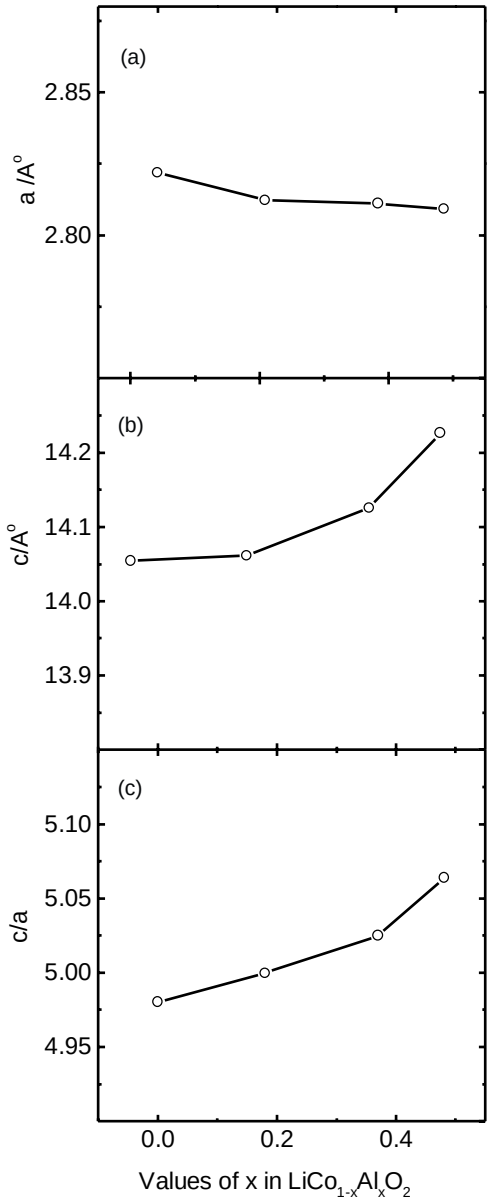

Fig. 3. Variation of lattice parameters with Al content.

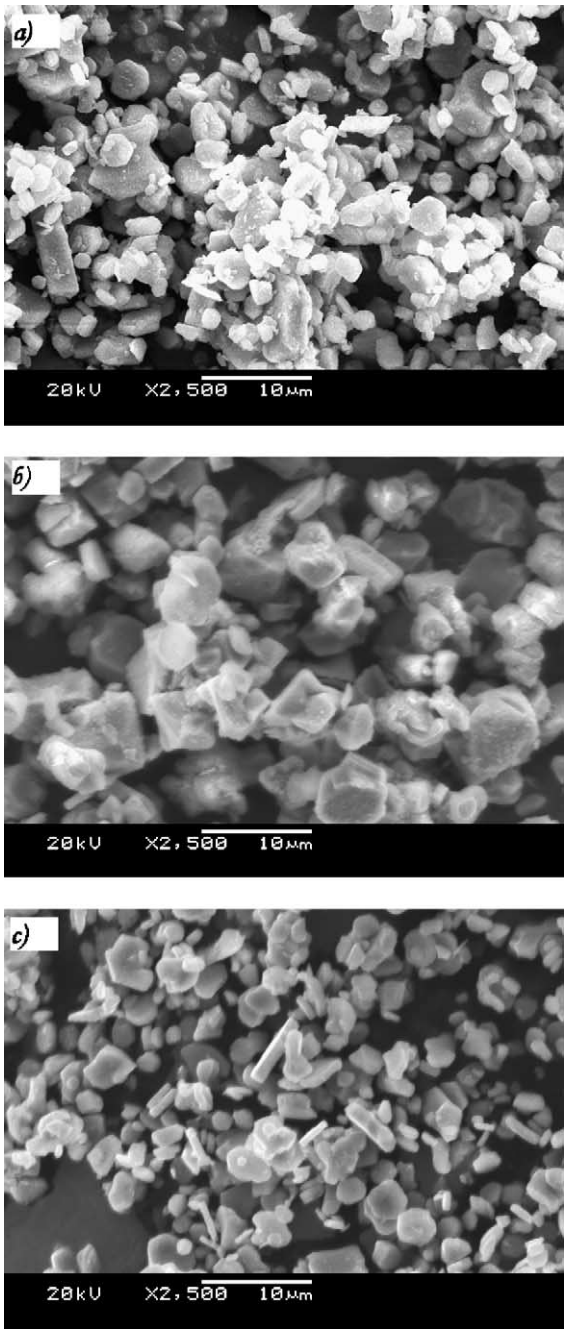

Fig. 4. Electron micrographs of (a) $LiCoO_2$; (b) $LiCo_{0.8}Al_{0.2}O_2$; and (c) $LiCo_{0.9}Mg_{0.1}O_2$.

After charging the Al doped samples to 4.2 V, the cells were allowed to equilibrate for 20 h and the open-circuit voltage (OCV) was measured (Fig. 7). The OCV increases with increase of Al in $LiCo_{1-x}Al_xO_2$, which thus supports the predictions of Ceder et al. [11]. Cycle-life data for $LiCo_{1-x}Al_xO_2$ of several compositions are presented in Fig. 8. The first discharge capacity of $LiCoO_2$ is as high as 125 mAh g^{-1}, and stabilizes at about 80 mAh g^{-1} after a few cycles. The average capacity is ~88 mAh g^{-1}, which is comparable with values reported in the literature [12,16].

It has been reported that Al substitution in $LiCoO_2$ leads to fading of discharge capacity upon cycling [11,12,16]. In the present study of $LiCo_{0.8}Al_{0.2}O_2$, the first discharge capacity is as high as 100 mAh g^{-1} and the capacity on the 10th cycle is 70 mAh g^{-1} (Fig. 8(b)). Thus, there is a 30% decrease of capacity by the end of 10 cycles. Nearly similar charge–discharge behavior is observed for $LiCo_{0.6}Al_{0.4}O_2$ (Fig. 8(c)). The average discharge capacity is 75 mAh g^{-1}. For the $LiCo_{0.5}Al_{0.5}O_2$ electrode (Fig. 8(d)), however, the value of the first discharge capacity (64 mAh g^{-1}) and the average discharge capacity (47 mAh g^{-1}) are found to be less than of $LiCo_{0.8}Al_{0.2}O_2$ and $LiCo_{0.6}Al_{0.4}O_2$ compositions. It is thus found that $LiCo_{(1-x)}Al_xO_2$ with $x = 0.2$ is a better than variants with $x > 0.2$, in terms of both discharge capacity and capacity retention. In the present case (i.e. $x =$

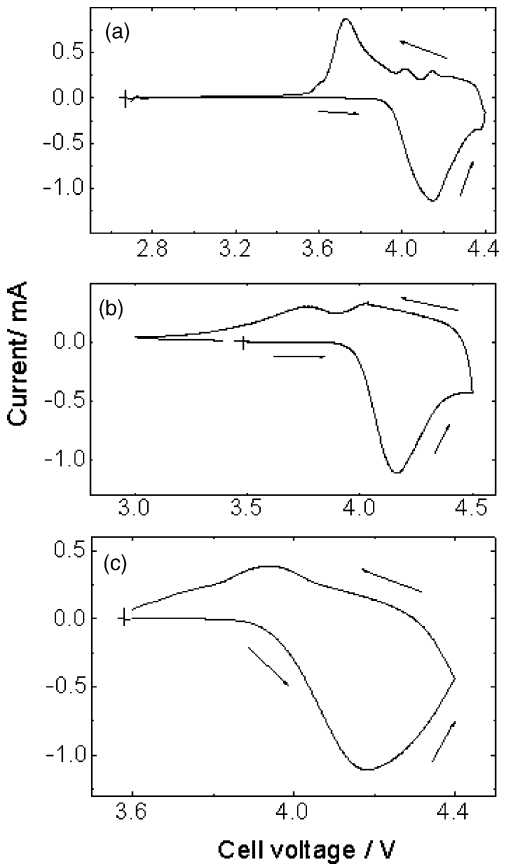

Fig. 5. Cyclic voltammograms for (a) $LiCoCO_2$ (wt. = 12 mg); (b) $LiCo_{0.8}Al_{0.2}O_2$ (wt. = 14 mg); and (c) $LiCo_{0.9}Mg_{0.1}O_2$ (wt. = 10 mg). Voltammograms recorded at scan rate of 50 $\mu V\,s^{-1}$.

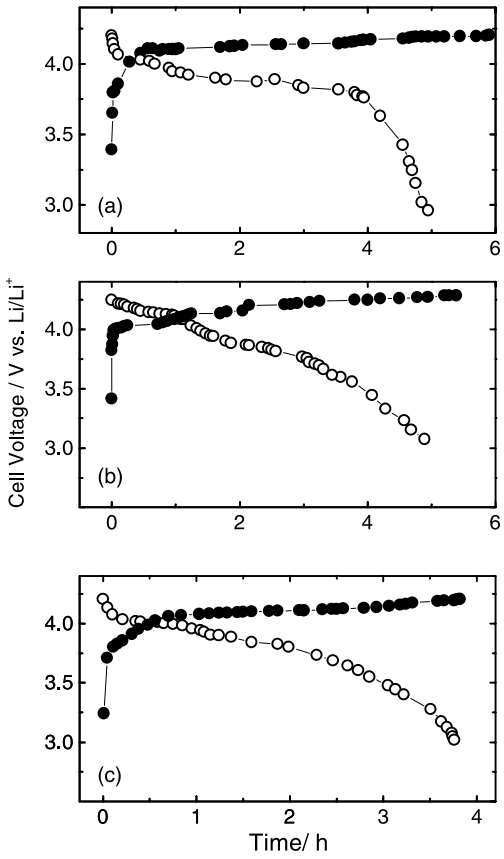

Fig. 6. Charge–discharge curves: (a) $LiCoO_2$ (11.6 mg); (b) $LiCo_{0.8}Al_{0.2}O_2$ (12.5 mg); and (c) $LiCo_{0.9}Mg_{0.1}O_2$ (12.6 mg) ((●) charging; (○) discharging; current = 200 μA).

0.2), the discharge capacity fading (30% after 10 cycles) is less than that reported in the literature [12]. Also, the average discharge capacity is 85 mAh g^{-1}, which is higher than that found by other workers [12,16]. The gradual decrease in discharge capacity as Al substitution is varied from 0.2 to 0.5 may be attributed to an increase in the occupation of Al^{3+} in the octahedral and tetrahedral environment [23].

Cycle-life data of $LiCo_{0.9}Mg_{0.1}O_2$ and $LiCo_{0.8}Mg_{0.2}O_2$ cells are also given in Fig. 8(e) and (f). The first discharge capacity of both the electrodes is as high as 130 mAh g^{-1}, but at the 10th cycle is only ~60 mAh g^{-1}. The average discharge capacity of $LiCo_{0.9}Mg_{0.1}O_2$ and $LiCo_{0.8}Mg_{0.2}O_2$ is 73 and 77 mAh g^{-1}, respectively.

3.3. Impedance spectroscopy

The impedance spectra of $LiCoO_2$ and $LiCo_{0.8}Al_{0.2}O_2$ cells in the Nyquist plot at various state-of-charge (SoC) values are shown in Fig. 9. Each spectrum is characterized by a semi-circle in the high-frequency region, and a spike in the low-frequency region. The semi-circle is attributed to the presence of a passivating film on the oxide surface [37–39]. The low-frequency spike is an arc of an incomplete semi-circle, which is attributed to the charge-transfer re-

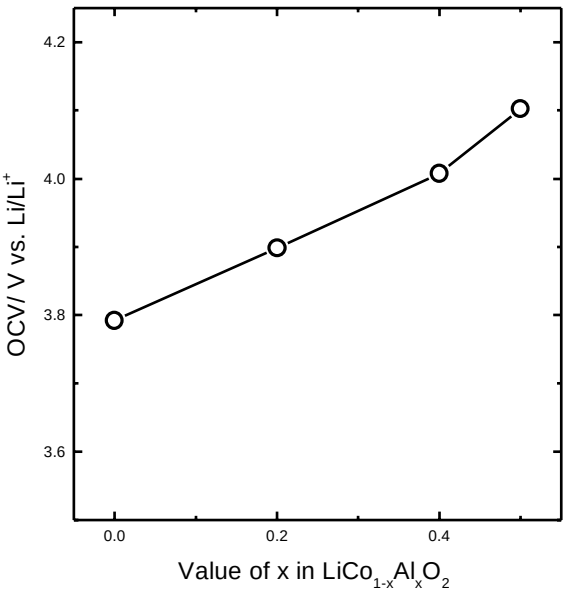

Fig. 7. Open-circuit voltage of $LiCo_{1-x}Al_xO_2$ cathodes.

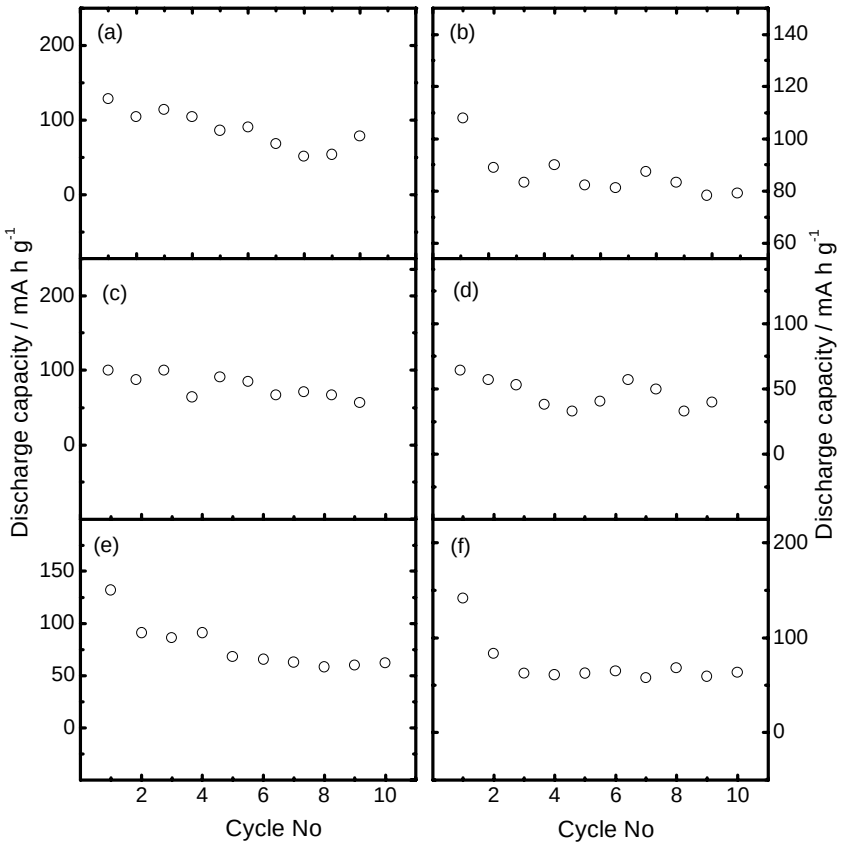

Fig. 8. Cycle-life data of (a) $LiCoO_2$; (b) $LiCo_{0.8}Al_{0.2}O_2$; (c) $LiCo_{0.6}Al_{0.4}O_2$; (d) $LiCo_{0.5}Al_{0.5}O_2$; (e) $LiCo_{0.9}Mg_{0.1}O_2$; and (f) $LiCo_{0.8}Mg_{0.2}O_2$.

sistance of electrochemical reaction. At high (SoC) values, the low-frequency part of the spectrum tends to become a semi-circle. Since more lithium ions are de-intercalated from the positive electrode, the diameter of the second semi-circle decreases due to an insulator-to-metal transition [39]. Similar behavior is observed for Mg-doped $LiCoO_2$ electrodes (not shown). For the purpose of evaluation of impedance parameters, an equivalent circuit $R(RQ)(RQ)$, where R represents a resistance and Q a constant phase element, is used, and parameters are obtained

Table 1
The ac impedance parameters of $LiCoO_2$[a]

SoC	R (Ω)	R_1 (Ω)	$Q_1 \times 10^5$ (Ω^{-1})	n_1	$R_{ct} \times 10^{-3}$ (Ω)	$Q_2 \times 10^3$ (Ω^{-1})	n_2
0	25	1×10^3	5.2	0.54	38.1	2.4	0.84
0.25	26	148	4.6	0.59	10.3	4.2	0.77
0.5	28	856	4.1	0.57	2.2	5.4	0.80
0.75	29	677	4.4	0.68	1.7	5.7	0.81
1	22	396	3.7	0.72	0.3	4.2	0.81

[a] The symbols are defined as follows: R, ohmic resistance; R_1, resistance of surface passive film corresponding to high-frequency semi-circle; Q_1, constant phase element in parallel to R_1; n_1, coefficient for Q_1; R_{ct}, charge-transfer resistance corresponding to low-frequency semi-circle; Q_2, constant phase element in parallel with R_{ct}; n_2, coefficient for Q_2.

Table 2
The ac impedance parameters of $LiCo_{0.8}Al_{0.2}O_2$

SoC	R (Ω)	R_1 (Ω)	$Q_1 \times 10^4$ (Ω^{-1})	n_1	$R_{ct} \times 10^{-3}$ (Ω)	$Q_2 \times 10^3$ (Ω^{-1})	n_2
0	52	263.7	2.1	0.62	4.8	4.6	0.79
0.25	47	94.0	1.4	0.48	1.7	7.2	0.80
0.5	50	83.9	1.7	0.55	1.6	7.3	0.75
0.75	43	75.4	1.9	0.47	1.1	8.0	0.79
1	44	73.8	1.8	0.47	0.9	8.2	0.80

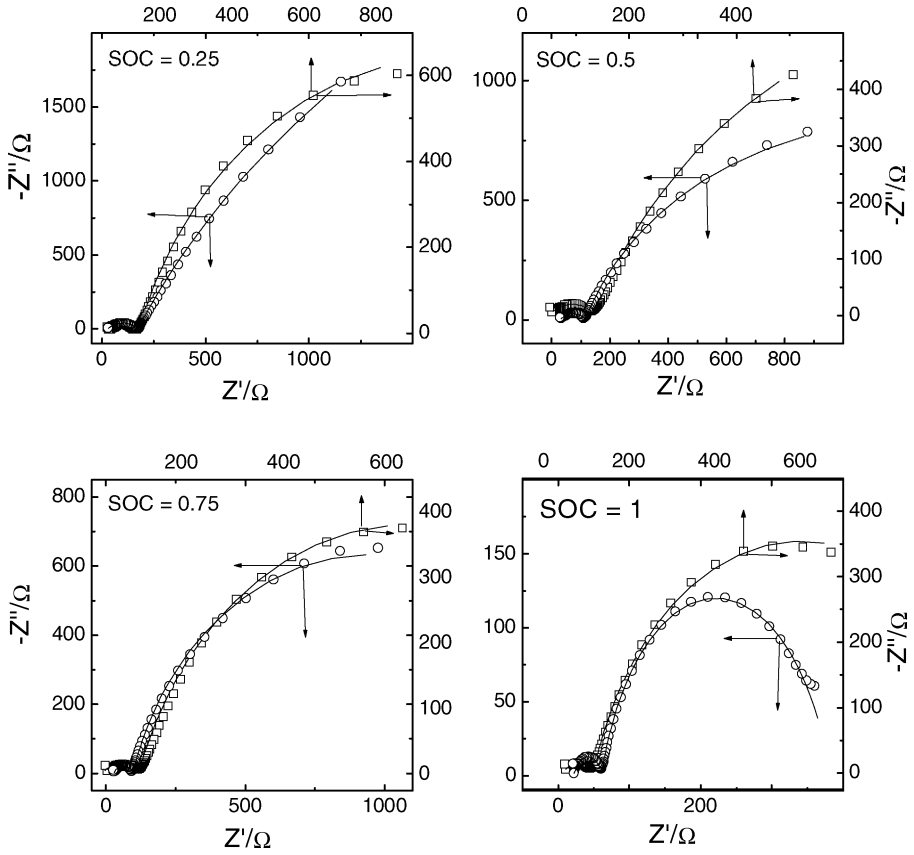

Fig. 9. The ac impedance plots of $LiCoO_2$ (○) and $LiCo_{0.8}Al_{0.2}O_2$ (□) at state-of-charge (SoC) values indicated. Experimental data shown by symbols and theoretical curves obtained from NLLS fitting by solid lines.

Table 3
The ac impedance parameters of $LiCo_{0.9}Mg_{0.1}O_2$

SoC	R (Ω)	$R_1 \times 10^{-4}$ (Ω)	$Q_1 \times 10^3$ (Ω^{-1})	n_1	$R_{ct} \times 10^{-3}$ (Ω)	$Q_2 \times 10^3$ (Ω^{-1})	n_2
0	18	1.52	2.1	0.62	4.1	4.6	0.55
0.25	18	1.15	3.84	0.95	3.4	2.4	0.63
0.5	17	1.13	1.94	0.71	1.58	4.1	0.59
0.75	16	2.25	2.07	0.65	1.04	4.88	0.57
1	19	1.0	2.43	0.66	1.03	5.48	0.56

from a non-linear, least-squares fitting procedure [38,39]. The impedance parameters of $LiCO_2$, $LiCo_{0.8}Al_{0.2}O_2$ and $LiCo_{0.9}Mg_{0.2}O_2$ electrodes are given in Tables 1–3, respectively. It is seen that R_{ct} decreases as the SoC increases. This study is in agreement with ac impedance studies of commercial lithium-ion cells and $LiCoO_2$ electrodes, for which a decrease in cell impedance with increase of SoC has been reported [38,39].

4. Conclusions

Gram quantities of single-phase $LiCo_{1-x}M_xO_2$ (M = Al and Mg) ($x = 0.5$ for Al and $x = 0.2$ for Mg) cathode materials for Li-ion batteries are synthesized by microwave dielectric heating within a short span of about 20 min. X-ray diffraction patterns of the prepared samples reveal a hexagonal layered structure with space group $R3$-m. The lattice constants vary with composition. The compounds are electrochemically active with good discharge capacity. Among the Al-substituted $LiCoO_2$ samples, that with $x = 0.2$ Al is the best composition since it gives high discharge capacity and good capacity retention.

Acknowledgements

Financial assistance received from the Department of Science and Technology (DST), Government of India, is gratefully acknowledged. One author (P.E.) thanks the Council

of Scientific and Industrial Research, Government of India, for the award of a senior research fellowship.

References

[1] G. Pistoia, Lithium Batteries, Elsevier, Amsterdam, The Netherlands, 1994.
[2] K. Ozawa, Solid State Ionics 69 (1994) 212.
[3] C.D.W. Jones, E. Rossen, J.R. Dahn, Solid State Ionics 68 (1994) 65.
[4] R. Stoyanova, E. Zhecheva, L. Zarkova, Solid State Ionics 73 (1994) 233.
[5] H. Kobayashi, H. Shigemura, M. Tabuchi, H. Sakaebe, K. Ado, H. Kageyama, A. Hirano, R. Kanno, M. Wakita, S. Morimoto, S. Nasu, J. Electrochem. Soc. 147 (2000) 960.
[6] M. Holzapfel, R. Schreiner, A. Ott, Electrochem. Acta 46 (2001) 1063.
[7] C. Delmas, I. Saadoune, A. Rougier, J. Power Source 43–44 (1993) 595.
[8] C. Delmas, I. Saadoune, Solid State Ionics 53–56 (1992) 370.
[9] K.-K. Lee, K.-B. Kim, J. Electrochem. Soc. 147 (2000) 1709.
[10] S. Madhavi, G.V. Subba Rao, B.V.R. Chowdari, S.F.Y. Li, J. Electrochem. Soc. 148 (2001) A1279.
[11] G. Ceder, Y.-M. Chiang, D.R. Sadoway, M.K. Aydinol, Y.-I. Jang, B. Huangy, Nature 392 (1998) 694.
[12] Y.-I. Jang, B. Huang, H. Wang, D.R. Sadoway, G. Ceder, Y.-M. Chiang, H. Liu, H. Tamura, J. Electrochem. Soc. 146 (1999) 862.
[13] J.D. Perkins, C.S. Bahn, P.A. Parilla, J.M. McGraw, M.L. Fu, M. Duncan, H. Yu, D.S. Ginley, J. Power Sources 81–82 (1999) 675.
[14] Y.-I. Jang, B. Huang, H. Wang, G.R. Maskaly, G. Ceder, D.R. Sadoway, Y.-M. Chiang, H. Liu, H. Tamura, J. Power Sources 81–82 (1999) 589.
[15] H. Huang, G.V. Subba Rao, B.V.R. Chowdari, J. Power Sources 81–82 (1999) 690.
[16] W.-S. Yoon, K.-K. Lee, K.-B. Kim, J. Electrochem. Soc. 147 (2000) 2023.
[17] C. Julien, G.A. Nazri, A. Rougier, Solid State Ionics 135 (2000) 121.
[18] W.-S. Yoon, K.-K. Lee, K.-B. Kim, J. Power Sources 97–98 (2001) 303.
[19] S.-T. Myung, N. Kumagai, S. Komaba, H.-T. Chung, Solid State Ionics 139 (2001) 47.
[20] H. Tukamoto, A.R. West, J. Electrochem. Soc. 144 (1997) 3164.
[21] J.M. McGraw, C.S. Bahn, P.A. Parilla, J.D. Perkins, D.W. Readey, D.S. Ginley, Electrochim. Acta 45 (1999) 187.
[22] E. Rossen, J.N. Reimers, J.R. Dahn, Solid State Ionics 62 (1993) 53.
[23] R. Alcantara, P. Lavela, P.L. Relano, J.L. Tirado, E. Zhecheva, R. Stoyanova, Inorg. Chem. 37 (1998) 264.
[24] S. Rodrigues, N. Munichandraiah, A.K. Shukla, J. Power Sources 102 (2001) 322.
[25] A.J. Berteaud, J.C. Badot, J. Microwave Power 11 (1976) 315.
[26] D.R. Baghurst, A.M. Chippindale, D.M.P. Mingos, Nature 332 (1988) 311.
[27] I. Ahmed, I.C. Dalton, D.E. Clark, J. Microwave Power Electromagnetic Energy 26 (1991) 128.
[28] D.M.P. Mingos, D.R. Baghurst, Br. Ceram. Trans. J. 91 (1992) 124.
[29] K.J. Rao, P.D. Ramesh, Bull. Mater. Sci. 18 (1995) 447.
[30] K.J. Rao, B. Vaidhyanathan, M. Ganguli, P.A. Ramakrishnan, Chem. Mater. 11 (1999) 882.
[31] H. Yan, X. Huang, Z. Lu, H. Huang, R. Xue, L. Chen, J. Power Sources 68 (1997) 530.
[32] H. Yan, X. Huang, L. Chen, J. Power Sources 81–82 (1999) 647.
[33] P.S. Whitfield, I.J. Davidson, J. Electrochem. Soc. 147 (2000) 4476.
[34] V. Subramanian, C.L. Chen, H.S. Chon, G.T.K. Fey, J. Mater. Chem. 11 (2001) 3348.
[35] P. Elumalai, H.N. Vasan, N. Munichandraiah, International Conference on Inorganic Materials for New Millennium (INMN), Indian Institute of Technology Madras, Chennai, India, January 2001.
[36] K. Dokko, M. Mohamedi, Y. Fujita, T. Itoh, M. Nishizawa, M. Umeda, I. Uchida, J. Electrochem. Soc. 148 (2001) A422.
[37] S. Rodrigues, N. Munichandraiah, A.K. Shukla, J. Solid State Electrochem. 3 (1999) 397.
[38] P. Suresh, A.K. Shukla, N. Munichandraiah, J. Appl. Electrochem. 32 (2002) 267.
[39] F. Corse, F. Nobili, A. Deptula, W. Lada, R. Tossici, A.D. Epifanio, B. Scrosati, R. Marassi, Electrochem. Comm. 1 (1999) 605.